

EVALUATION OF DIFFERENT TURBULENCE APPROACHES TO PREDICT THE FLOW INSIDE A DESIGNED HIGH OIL HYDROCYCLONE

G.M. Raposo, gelmirez@petrobras.com.br

Petrobras / PCM / PROJ - Engineering depart., 22453-900 Macaé, RJ, Brazil

A. O. Nieckele, nieckele@puc-rio.br

Dept. of Mechanical Engineering – PUC/Rio, 22453-900 Rio de Janeiro, RJ, Brazil

Abstract. *Development of small size and weight separation equipment are crucial for the petroleum off-shore exploration. Since centrifugal fields are several times stronger than the gravity field, cyclonic separation has become very important as a unit process for gas-liquid, liquid-liquid and solid-liquid separation. The major difference between the various cyclones is their geometry. Cyclone optimization for different uses is, every year, less based on experiments and more based on mathematical models. In the present work, the flow field inside high oil content hydrocyclones is numerically obtained with FLUENT. The performance of the RANS turbulence model, Reynolds Stress Model (RSM), and a Large Eddy Simulation (LES), with Smagorinsky sub-grid model, is investigated to predict the flow inside a high oil content hydrocyclone. The results are compared with experimental data available in the literature. All models over-predicted the tangential component, especially at the reverse cone region. However, the prediction of the tangential turbulent fluctuations with LES was significant better than the RSM prediction.*

Keywords: *Cyclonic separation, hydrocyclone, RSM turbulence model, LES, numerical simulation.*

1. INTRODUCTION

Hydrocyclone are devices to separate fluids with different densities under a strong centrifugal field. The continuum phase is liquid and the other one is disperse. Hydrocyclones, that do not have rotating parts, induce this field by channelling the flow passing through it.

Cyclonic separation has been used for more than a century in the industry. Hydrocyclones for solid/ liquid separation were patent by the first time by Bretney at 1891 (Chiné and Concha, 2000), and the “de-oiling” hydrocyclone for liquid/ liquid separation was patented at 1978, applied to water treatment in Oil Industry (Young et al., 1994). This application used a very disperse oil phase (less than 1% in volume, v/v). Recent researches are looking for equipment able of handling high oil contents, up to 50% v/v, as long as water remains the continuous phase.

Application of cyclone or hydrocyclone in the oil industry has been growing; since it can reduce significantly the time and cost required for separating phases (oil, water, gas, solid particles), especially, for off-shore production, where small size and weight are crucial design parameters.

Hydrocyclones are different from each other basically on geometric parameters such as inlet diameter, cyclone diameter, length and angles of conical sections. The design of a hydrocyclones used to be based on empirical correlations, however, during the last years numerical simulations has been used to help the design and a large number of publication can be found (Daí et al, 1999; Melo et al, 2003, Matvienko, 2004, Narasimha et al, 2006, Bhaskar et al, 2007; Husveg et al, 2007). In spite of the large number of papers, only a few data are available concerning water/oil separation, since the oil industry does not always allow disclosure of their research.

Performance improvement, which relies on geometric changes, is every year less dependent on experimental work with real prototypes and more based on computational fluid dynamics (CFD) simulation work. Nowakowski (2004) presents a review of hydrocyclones numerical simulation evolution, which is strongly related with computer capacity and the development of turbulence models. It was started with two dimensions models (2D) evolving to three dimensions (3D) and from stationary to transient in time flow simulation. Because flow inside hydrocyclones is highly turbulent, the modelling of turbulence is crucial. Turbulence has been modelled with algebraic methods, two equations methods like κ - ϵ , RSM (Reynolds Stress Models) and LES (Large Eddy Simulation).

Several references (Montavon et al, 2000; Olson et al, 2004) have reported that the hydrocyclone flow predictions with RSM turbulence models are superior to the κ - ϵ simulation results. In spite of the large cost, the modelling of turbulence employing LES has been increasing in a number of practical applications (Narasimha et al, 2006; Brennan et al, 2007).

At the present work, the flow field is numerically obtained for a hydrocyclone design for high oil content application, employing the commercial code FLUENT. The results are compared with available experimental data (Marins, 2007), acquired both PIV (Particle Image Velocimetry) and LDV (Laser Doppler Velocimetry) techniques for the same hydrocyclone. Two different approaches to predict the turbulent flow are analyzed: Reynolds Stress Model (RSM) and Large Eddy Simulation (LES), employing the Smagorinsky sub-grid model. Tangential and axial velocity profiles are examined, as well as the turbulence intensity.

2. MATHEMATICAL MODELING

The geometric model for the 70 mm diameter hydrocyclone used is illustrated in Fig. 1. This equipment shows two tangential inlets followed by a short high angle cone that causes acceleration on tangential velocities based on angular momentum conservation. It has a long short angle cone that balances energy dissipation, giving more time for phase separation. Finally, there is a cylinder to connect with the underflow (heavy phase) outlet. On the top of the hydrocyclone is located de reject (light phase) outlet.

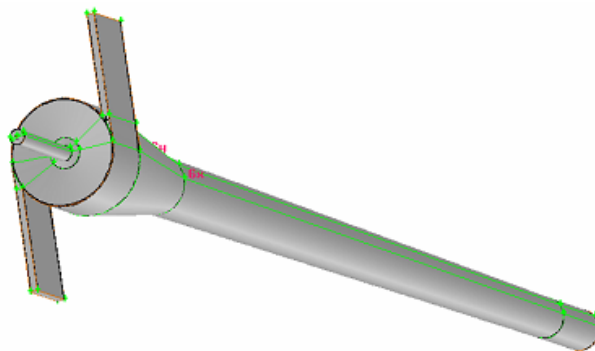


Figure 1 – Geometric model used on hydrocyclone model

Inside the hydrocyclone the flow develops into a combination of two vortices. The first one is located close to axial line with a tangential velocity profile similar to a solid body rotation, where tangential velocity increases with radius. After the maximum, the tangential velocity profile behaves as a free vortex until it reaches the wall, where tangential velocity is inversely proportional to radius, decreasing to zero close to wall. This tangential velocity profile establishes the centrifugal field and is balanced by a pressure profile that has a minimum over the axial line. This low pressure promotes a reversion on central flow allowing the split into reject and underflow outlets.

The transport equations that describe conservation of momentum and mass for a single phase, incompressible flow are respectively the Navier-Stokes and continuity equations, which read:

$$\rho \left[\frac{\partial u_i}{\partial t} + \frac{\partial (u_j u_i)}{\partial x_j} \right] = - \frac{\partial p}{\partial x_i} + \mu \frac{\partial^2 u_i}{\partial x_j^2} \quad ; \quad \frac{\partial u_j}{\partial x_j} = 0 \quad (1)$$

with u_i the velocity component, p the pressure, ρ the fluid density, and μ the dynamic viscosity.

The RSM method is based on Reynolds average concept, where $u_i = \overline{u_i} + u'_i$ and $\overline{u_i}$ is the time average velocity and u'_i is the velocity fluctuation. The principle behind LES is that larger turbulent eddies are resolved as part of a dynamic integration of the equations of motion but the eddies that are smaller than the grid are not resolved and the momentum transfer due to these subgrid scale eddies is modeled. For the LES formulation, $\overline{u_i}$ is the resolved velocity and u'_i is the filtered velocity. The resulting average and filtered momentum equation can be written as:

$$\rho \left[\frac{\partial \overline{u_i}}{\partial t} + \frac{\partial (\overline{u_j u_i})}{\partial x_j} \right] = - \frac{\partial \overline{p}}{\partial x_i} + \mu \frac{\partial^2 \overline{u_i}}{\partial x_j^2} + \frac{\partial (\tau_{ij})}{\partial x_j} \quad (2)$$

where the new term τ_{ij} that appears in the momentum equation is modeled in different ways for each approach.

2.1. Reynolds Stress Model

The Reynolds stress tensor $\tau_{ij} = \rho \overline{u'_i u'_j}$ is determined by the solution of its transport equations:

$$\left[\frac{\partial \rho \overline{u'_i u'_j}}{\partial t} + \frac{\partial (\overline{u_j \rho \overline{u'_i u'_j}})}{\partial x_j} \right] = \frac{\partial}{\partial x_j} \left[\left(\mu + \frac{\mu_t}{\sigma_\kappa} \right) \frac{\partial \overline{u'_i u'_j}}{\partial x_j} \right] + P_{ij} + \phi_{ij} - \frac{2}{3} \rho \varepsilon \delta_{ij} + F_{ij} \quad (3)$$

where ϕ_{ij} is the pressure strain correlation of turbulence, based on the quadratic model SSG (Speziale et al. , 1991), P_{ij} is the production term of the Reynolds stress and F_{ij} is the production due to the rotation ω_k , given by

$$P_{ij} = - \left(\rho \overline{u'_i u'_k} \frac{\partial \overline{u_j}}{\partial x_k} + \rho \overline{u'_j u'_k} \frac{\partial \overline{u_i}}{\partial x_k} \right) ; \quad F_{ij} = -2 \rho \omega_k \left(\overline{u'_i u'_k} \epsilon_{ikm} + \overline{u'_j u'_k} \epsilon_{jkm} \right) \quad (4)$$

where ϵ_{ijk} is the permutation symbol (Levi-Civita) and δ_{ij} is Kronecker delta. $\sigma_\kappa = 1$ is an empirical constant and ϵ is the turbulence dissipation and can be obtained from its conservation equation, as employed in the κ - ϵ model

$$\left[\frac{\partial \rho \epsilon}{\partial t} + \frac{\partial (\overline{u_j \rho \epsilon})}{\partial x_j} \right] = \frac{\partial}{\partial x_j} \left[\left(\mu + \frac{\mu_t}{\sigma_\epsilon} \right) \frac{\partial \epsilon}{\partial x_j} \right] + c_{1\epsilon} \frac{\epsilon}{\kappa} P - c_{2\epsilon} \frac{2}{3} \rho \frac{\epsilon}{\kappa} \quad (5)$$

where $P = 0.5 P_{ii}$ is the production term, and the empirical constants are: $\sigma_\epsilon = 1.0$; $c_{1\epsilon} = 1.44$; $c_{2\epsilon} = 1.92$. The turbulent kinetic energy κ can be obtained from the trace of the Reynolds stress tensor.

2.2. Large Eddy Simulation

With the LES approach the additional term τ_{ij} in Eq. (2) is the sub-grid tensor,

$$\tau_{ij} = - \left(\overline{u_i u_j} - \overline{u_i} \overline{u_j} \right) \quad (6)$$

and it can be modeled according to Smagorinsky, (1963) as

$$\tau_{ij} - \frac{1}{3} \tau_{ii} \delta_{ij} = 2 \mu_t \overline{S_{ij}} \quad ; \quad \overline{S_{ij}} = \frac{1}{2} \left[\frac{\partial \overline{u_i}}{\partial x_j} + \frac{\partial \overline{u_j}}{\partial x_i} \right] \quad (7)$$

where the subgrid turbulent viscosity μ_t is

$$\mu_t = \rho L_s^2 \left| \overline{S} \right| \quad , \quad L_s = \min \left(k d, C_s \forall^{1/3} \right) \quad (8)$$

$|\overline{S}|$ is the trace of the deformation tensor S_{ij} , $k=0.4187$ is the von Karmán constant, d is the distance to the closest wall, the Smagorinsky constant $C_s=0.1$ and \forall is the element control volume.

2.3. Near wall region

Special modeling was employed at the near wall regions for both approach. The standard “wall function” was employed for LES cases while a parameter ΔB was included to consider the wall roughness. :

$$\frac{u C_\mu^{1/4} \kappa^{1/2}}{\tau_w / \rho} = \frac{1}{k} \ln \left(E \frac{\rho C_\mu^{1/4} \kappa^{1/2} y}{\mu} \right) - \Delta B \quad (9)$$

where τ_w is the wall shear stress and $C_\mu = 0.09$. The term ΔB is a function of the roughness and it was modeled based on a dimensionless roughness height, K_s^+ , defined as:

$$K_s^+ = \rho K_s u^* / \mu, \quad u^* = C_\mu^{1/4} \kappa^{1/2} \quad (10)$$

There are three correlations for ΔB as a function de K_s^+ , corresponding to a smooth pipe, transition and totally rough pipe, as

$$\Delta B = 0 \quad \text{for } K_s^+ \leq 2.25 \quad (11)$$

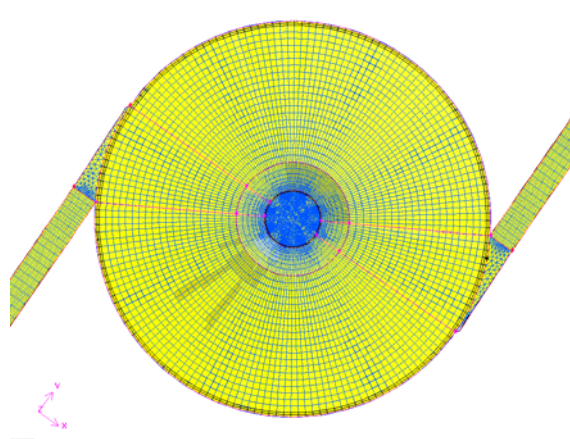
$$\Delta B = \frac{1}{k} \ln \left[\frac{K_s^+ - 2.25}{87.75} + C_s K_s^+ \right] \times \sin \left[0.4258 (\ln K_s^+ - 0.811) \right]. \quad \text{for } 2.25 < K_s^+ < 90 \quad (12)$$

$$\Delta B = \frac{1}{k} \ln \left[1 + C_s K_s^+ \right]. \quad \text{for } K_s^+ > 90 \quad (13)$$

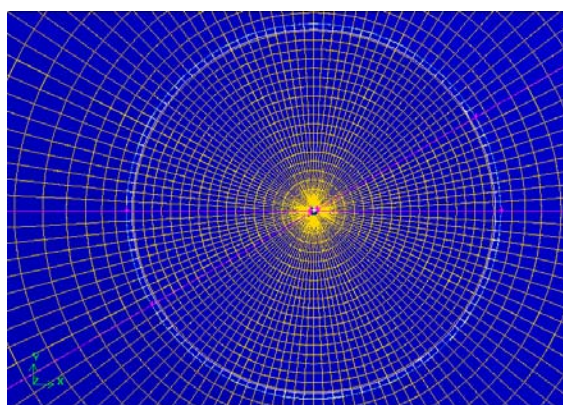
The empirical constant C_s was set as 0.5. For the RSM cases, the wall function was also modified to include corrections due to pressure gradients (Kim e Choudhury, 1995)

3. NUMERICAL METHOD

The conservation equations were numerically solved with FLUENT, in a domain with one million cells. A top view from the meshed volume into hexaedric cells is presented on Fig. 2a. Better results, avoiding numeric inconsistencies were obtained creating a virtual cylinder (0.2 mm diameter) around the central axial line of the hydrocyclone under a “no shear” boundary condition. This gave us better a cell quality as indicated in Fig. 2b.



(a) Top view



(b) Detail over virtual cylinder in the middle of the meshed volumes.

Figure 2. Meshed domain. (a) Top view. (b) Detail over virtual cylinder in the middle of the meshed volumes.

It was employed a second order time integration, the second order *Upwind* (Fluent, 2008) and QUICK (Leonard, 1979) schemes for the spatial discretization. PRESTO (Fluent, 2008) was used for pressure calculations. SIMPLE (Patankar, 1980) was chosen for pressure-velocity coupling. For the solution of the algebraic linear system it was applied Gauss-Siedel with AMG method (Hutchinson, B. R.; Raithby, G. D., 1986).

4. RESULTS

To allow comparison with the experimental data, water flow rate equal to $6.2 \text{ m}^3/\text{h}$ was imposed, with a split of 35% to the overflow and 65% to the underflow. 10 % turbulence intensity was specified at the inlet with a 4.8 mm of characteristic length.

Results are presented over radius lines and surfaces referenced to reject as indicated in Fig. 3.

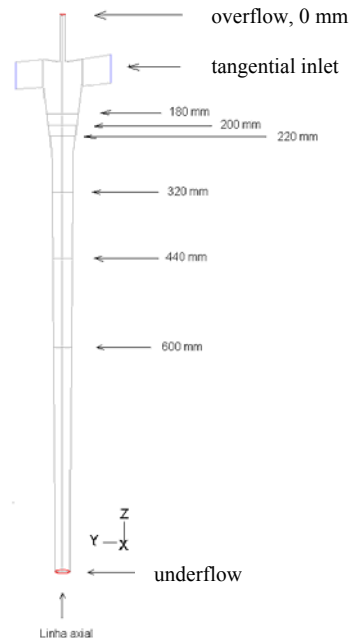


Figure 3 Reference lines for profiles in the hidrocyclone

The influence in the prediction of axial and tangential velocity, employing two different approaches to predict the turbulence flow (RSM and LES), as well as two discretization schemes (2nd order Upwind and QUICK), are analyzed, by comparing with the experimental data of Marins (2007). The QUICK scheme was employed with LES and RSM, while the 2nd order Upwind was only employed with the RSM model.

Figure 4 presents the tangential velocity profile along a radial position at four cross sections (as shown in Fig. 3). Two cross sections located near the inlet, at the position equal to 180 mm and 220 mm, one at the mid section at 440 mm and the last one near the underflow at 600 mm.

Analyzing the tangential velocity profiles in Fig. 4, it can be seen that qualitatively all models predicted the correct flow behavior. Near the walls there is a strong gradient and near the center, at the core region, another steep gradient can be seen with the tangential velocity dropping to almost zero. Note however, in Fig. 4, that all models have super estimated the tangential velocity profiles. RSM (2nd Upwind) has also over predicted the central gradient and RSM (QUICK) under predict it. LES results were closer to experimental data, although, maximum tangential velocity was highly over estimated. Outside the central core, as one approach the walls, all cases have converged to approximate same results, with the same slope as the experimental case, although displaced.

Far from the inlet (at the position 600 mm), at the narrower region, approximately the same flow behavior was predicted, as it can be seen in Fig. 4d. A possible cause for the discrepancy can be the use of the “wall functions”, which by forcing the wall gradient causes an increase in the velocity.

At the same axial position selected to analyze the tangential components, the axial velocity component are plotted along the radius at Fig. 5. Once again all models predicted qualitatively the correct flow development along the hydrocyclone. Near the overflow, high upstream axial velocities are observed at the central cone. As one move along the hydrocyclone, the peak velocity of the reverse cone is slightly reduced, and the cone diameter is kept approximately constant. Note also that as the cone gets narrower, the downstream flow increases in intensity. It can be seen in Fig. 5 that near the entrance, all models were able to foresee the reverse cone size (diameter) flowing to overflow. But, no model was able to predict the maximum axial velocity measured experimentally. RSM (2nd Upwind) showed the best results, followed by LES and RSM (Quick).

At the lower axial position (600 mm) at Fig. 5d it can be seen that a better prediction of the maximum velocity was obtained with the RSM model, with both discretization schemes. The LES result deteriorated, since it presented a wider central cone, with smaller velocities, and as a consequence larger negative velocities were obtained.

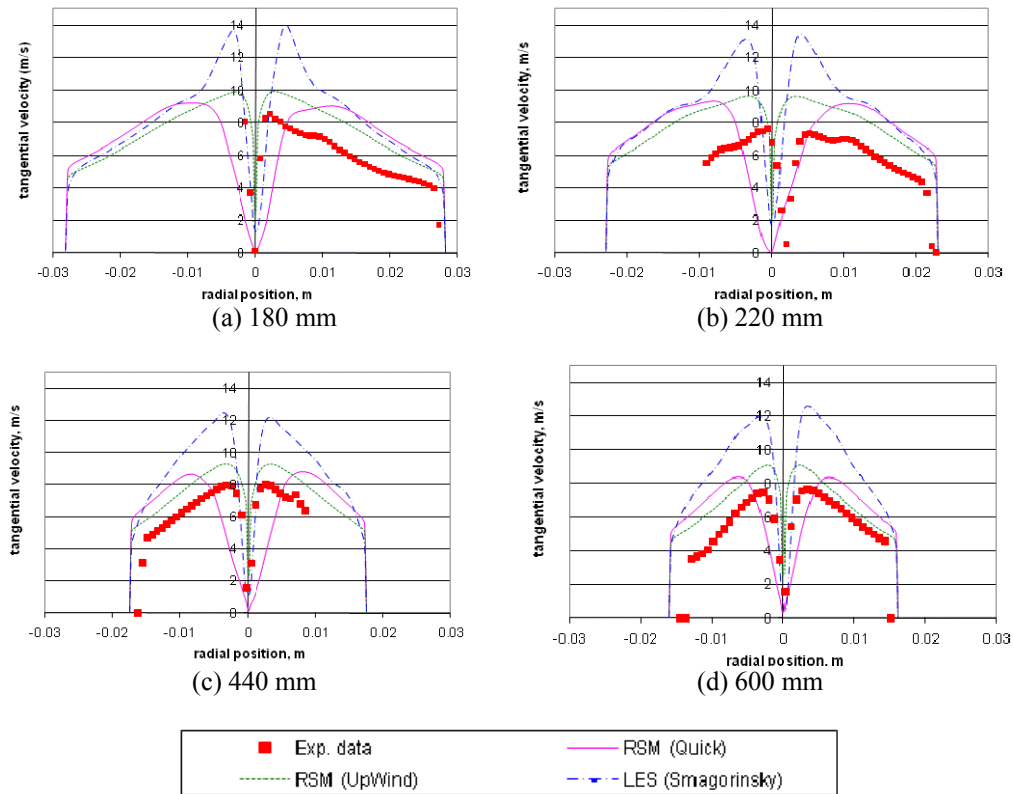


Figure 4 Tangential profiles versus radius. (a) section 180 mm (b) section 220 mm (c) section 440 mm (d) section 600 mm

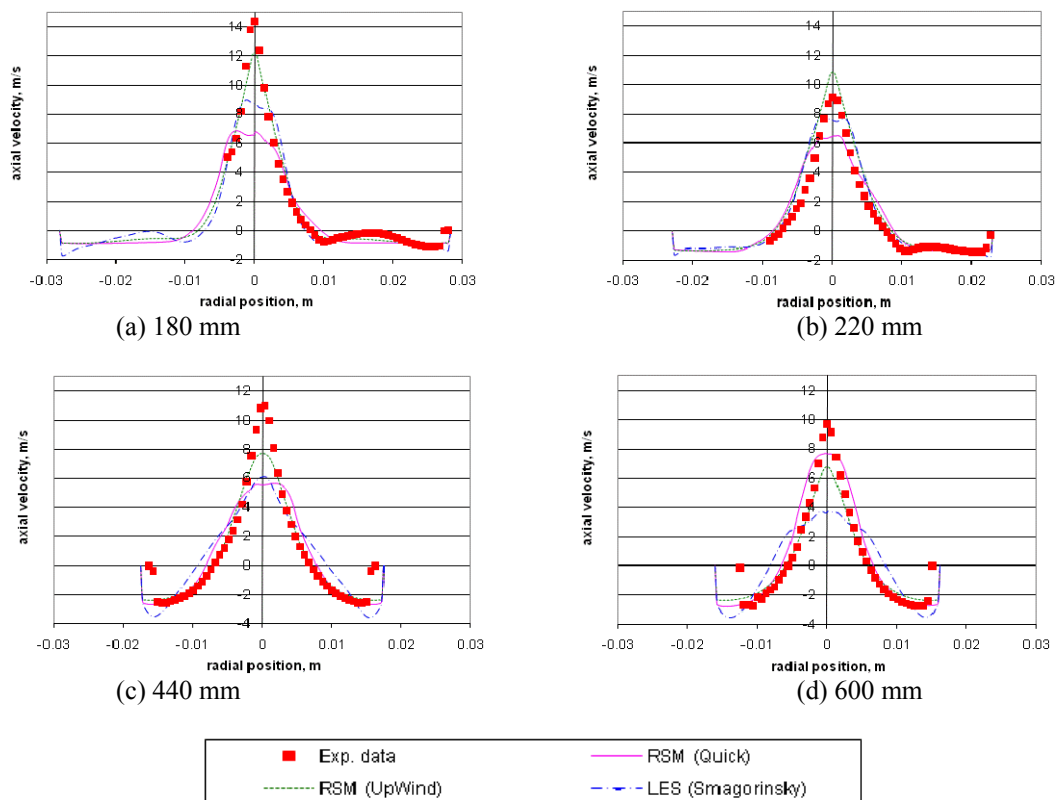


Figure 5 Axial profiles versus radius. (a) section 180 mm (b) section 220 mm (c) section 440 mm (d) section 600 mm

The turbulence intensity can be defined as the ratio between the velocity fluctuation and the mean velocity (norm $rms(v')/V$). Marins (2007) measured the velocity fluctuations components at the axial position equal to 400 mm and radial equal to 11.9 mm. The tangential component fluctuation was equal to 30% of the mean value. Figure 6 illustrate the fluctuations normalized by the mean value for the tangential component. Note that the LES results are quite superior to the RSM results, with a much higher value of turbulence intensity, approximately of the same order as the experimental data.

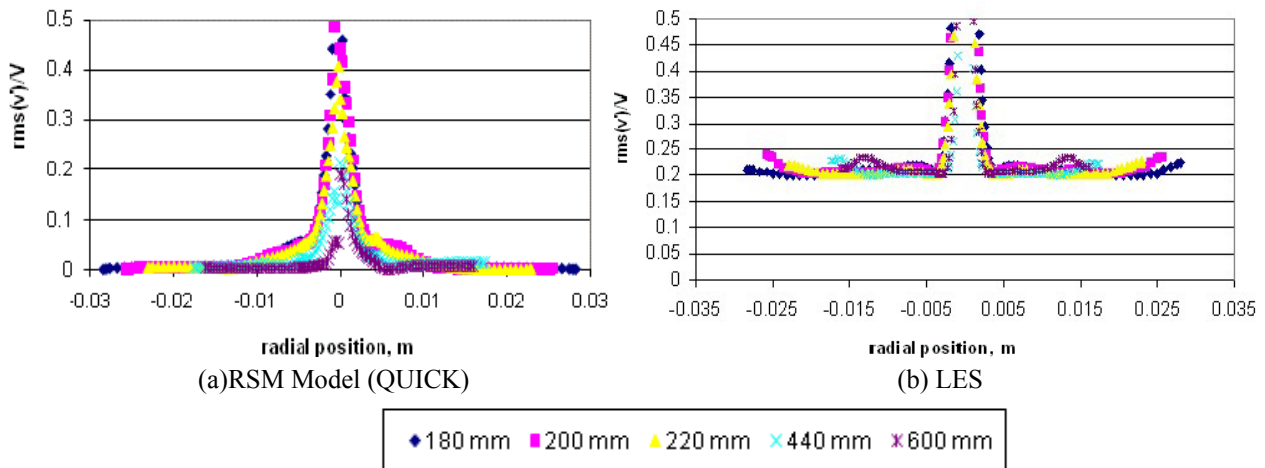


Figure 6: Tangential turbulent intensity

Table 1 presents the pressure difference between inlet and underflow obtained with all models. It can be seen that the pressure difference is larger when a higher tangential velocity is obtained, therefore, it can be said that there is a direct relation between pressure difference and tangential velocity component

Table 1 – Pressure difference between inlet and underflow.

Case	Pressure difference (bar)
RSM (QUICK)	0.631
RSM (2nd <i>Upwind</i>)	0.654
LES	0.687

The influence of the roughness in the pressure difference between inlet and underflow predicted with the RSM model is shown in Table 2, where it can be seen that the roughness induces a reduction in the pressure difference in according with experimental observation.

Table 2: Roughness influence in the pressure difference between inlet and underflow with RSM model.

Roughness ϵ (μm)	Pressure difference (bar)
RSM (QUICK) Smooth	0.631
RSM (QUICK) 50	0.493

5. FINAL REMARKS

The centrifugal forces present in a hydrocyclone are due to the tangential component; therefore the tangential component plays a more important role in the performance of the equipment. Both approaches employed to represent the turbulence flow (RSM and LES) presented some difficulty of predicting accurately the experimental data, however, both presented reasonable results for the tangential velocity profiles, closer to the inlets (180 mm).

Pressure drop results were as expected since most part of energy dissipation occurs around the reversed vortex, therefore the wall roughness increases the velocity gradient near the wall, but induces a reduction on velocity gradient at the core edge leading to a reduction on pressure difference.

6. ACKNOWLEDGEMENTS

The authors thank L.P. Marins and Petrobras Research Center (Cenpes) for experimental data and ESSS for its technical support over Fluent package. The second author also thanks the Brazilian Research Council, CNPq, for the support awarded to this work.

7. REFERENCES

- Bhaskar, K. U.; Murthy, Y. R.; Raju, M. R.; Tiwari, S.; Srivastava, J. K.; Ramakrishnan, N.; 2007, "CFD Simulation And Experimental Validation Studies On Hydrocyclone ", Minerals Engineering, Vol. 20, pp. 60-71
- Brennan, M.S.; Narasimha, M.; Holtham, P.N.; 2007. "Multiphase Modelling Of Hydrocyclones – Prediction Of Cut-Size", Minerals Engineering, Vol. 20, pp. 395-406.
- Cecebi, T.; Bradshaw, P.; 1977. Momentum Transfer in Boundary Layers. Hemisphere Publishing Corporation, New York.
- Chiné, B.; Concha, 2000, "Flow Patterns In Conical And Cylindrical Hydrocyclones", Chemical Engineering Journal, Vol. 80, pp. 267-273.
- Daí, G.Q.; Li, J.M.; Chen, W.M., 1999, "Numerical Prediction Of The Liquid Flow Within A Hydrocyclone", Chemical Engineering Journal, Vol. 74, pp. 217-223
- Fluent, 2008. Users guide.
- Husveg, T.; Rambu, O.; Drengstig, T.; Bistad, T.; 2007, "Performance Of Deoiling Hydrocyclone During Variable Flow Rates", Minerals Engineering. Vol. 20 (4), pp. 368-379.
- Hutchinson, B. R.; Raithby, G. D.. 1986, "A Multigrid Method Based on the Additive Correction Strategy", Numerical Heat Transfer, Vol. 9, pp. 511-537
- Kim, S.-E.; Choudhury, D; 1995. "A Near-Wall Treatment Using Wall Functions Sensitized to Pressure Gradient", In ASME FED Vol. 217, Separated and Complex Flows. ASME.
- Leonard, B. P., 1979. "A Stable Accurate Convective Modeling Procedure Based On Quadratic Upstream Interpolation", Computer methods in Appl. Mechanics and Engineering, Vol. 19, pp. 59–88.
- Marins, L. P., 2007, "Experimental Characterization Of The Flow Inside A Hydrocyclone Without A Gas Nucleus", in Portuguese, COPPE, Rio de Janeiro, Brazil
- Matvienko O.V., 2004, "Analysis of Turbulence Models and Investigation of the Structure of the Flow in a Hydrocyclone", Journal of Engineering Physics and Thermophysics, Vol. 77 (2), pp. 316-323, Springer
- Melo M.V.; Sant'anna Jr G.L.; Massarani G., 2003, "Flotation Techniques for Oily Water Treatment", Environmental Technology, Vol. 24 (7), pp. 867-876, Selper Ltd
- Montavon, C.A.; Grotjans, H.; Hamill, I.S., Phillips, H.W.; Jones, I.P., 2000. "Mathematical Modeling And Experimental Validation Of Flow In A Cyclone", Abstract for BHR Conference on Cyclone Technologies, Warnick 31 May-2 June
- Narasimha, M.; Brennan, M. S.; Holtham, P. N., 2006, Large Eddy Simulation Of Hydrocyclone- Prediction Of Air-Core Diameter And Shape", Int. J. Miner. Process., Vol. 80, pp. 1-14
- Nowakowski, A.F; Culivan J.C.; Williams R.A; Dyakowski T.; 2004. "Application Of Cfd To Modelling Of The Flow In Hydrocyclones. Is This A Realizable Option Or Still A Research Challenge? ", Minerals Engineering, 17, pp. 661-669
- Olson, T.J., Van Ommen, R., 2004. "Optimizing Hydrocyclone Design Using Advanced CFD Model", Minerals Engineering, Vol. 17, pp. 713-720.
- Patankar, S. V., 1980. Numerical Heat Transfer And Fluid Flow. Hemisphere, New York.
- Smagorinsky, J.; 1963. "General Circulation Experiments with the Primitive Equations. I. The Basic Experiment", Month. Wea. Rev., Vol. 91: pp. 99-164.
- Speziale, C.G.; Sakar, S.; Gatski, T.B., 1991. "Modelling The Pressure Strain Correlation Of Turbulence: An Invariant Dynamical Systems Approach", J. Fluid Mech, Vol. 227, pp. 245-272.
- Young, G.A.B; Wakley, W.D.; Taggart, D.L.; Andrews, S.L ; Worrel, J.R., 1994. "Oil-Water Separation Using Hydrocyclones: An Experimental Search For Optimum Dimensions", Journal of Petroleum Science and Engineering, Vol. 11, pp. 37-50.

8. RESPONSIBILITY NOTICE

The authors are the only responsible for the printed material included in this paper.